

RESEARCH ARTICLE | *Neural Circuits*

## A circuit for saccadic suppression in the primate brain

Rebecca A. Berman, James Cavanaugh, Kerry McAlonan, and Robert H. Wurtz

Laboratory of Sensorimotor Research, National Eye Institute, National Institutes of Health, Bethesda, Maryland

Submitted 24 August 2016; accepted in final form 21 December 2016

**Berman RA, Cavanaugh J, McAlonan K, Wurtz RH.** A circuit for saccadic suppression in the primate brain. *J Neurophysiol* 117: 1720–1735, 2017. First published December 21, 2016; doi:10.1152/jn.00679.2016.—Saccades should cause us to see a blur as the eyes sweep across a visual scene. Specific brain mechanisms prevent this by producing suppression during saccades. Neuronal correlates of such suppression were first established in the visual superficial layers of the superior colliculus (SC) and subsequently have been observed in cortical visual areas, including the middle temporal visual area (MT). In this study, we investigated suppression in a recently identified circuit linking visual SC (SCs) to MT through the inferior pulvinar (PI). We examined responses to visual stimuli presented just before saccades to reveal a neuronal correlate of suppression driven by a copy of the saccade command, referred to as a corollary discharge. We found that visual responses were similarly suppressed in SCs, PI, and MT. Within each region, suppression of visual responses occurred with saccades into both visual hemifields, but only in the contralateral hemifield did this suppression consistently begin before the saccade (~100 ms). The consistency of the signal along the circuit led us to hypothesize that the suppression in MT was influenced by input from the SC. We tested this hypothesis in one monkey by inactivating neurons within the SC and found evidence that suppression in MT depends on corollary discharge signals from motor SC (SCi). Combining these results with recent findings in rodents, we propose a complete circuit originating with corollary discharge signals in SCi that produces suppression in visual SCs, PI, and ultimately, MT cortex.

**NEW & NOTEWORTHY** A fundamental puzzle in visual neuroscience is that we frequently make rapid eye movements (saccades) but seldom perceive the visual blur accompanying each movement. We investigated neuronal correlates of this saccadic suppression by recording from and perturbing a recently identified circuit from brainstem to cortex. We found suppression at each stage, with evidence that it was driven by an internally generated signal. We conclude that this circuit contributes to neuronal suppression of visual signals during eye movements.

corollary discharge; macaque; suppression

SACCADIC SUPPRESSION IS THE REDUCTION in sensitivity to the visual stimuli swept across the retina during saccades. This reduced sensitivity is thought to contribute to our stable vision by removing the blur during saccades and thereby promoting a smooth perceptual transition from the presaccadic image to the postsaccadic image. The perceptual phenomenon of saccadic suppression is thought to arise from two primary sources. The first is a corollary discharge (CD) of each saccade, a copy of

the command for the impending movement. This extraretinal signal suppresses visual activity generated by the sweep of the retina across a visual scene. Consistent with an internally driven CD signal being its origin, perceptual suppression has been shown to begin before the eye starts to move (Latour 1962; Diamond et al. 2000). The second source of saccadic suppression is a visual masking mechanism; high-contrast images before and after the saccade mask the lower contrast blur during saccades (for further discussion of CD and masking mechanisms, see reviews by Wurtz 2008; Krekelberg 2010; Ibbotson and Krekelberg 2011; and Krock and Moore 2014). CD and masking together are so effective in suppressing visual input during saccades that the effect might better be referred to as saccadic omission (Campbell and Wurtz 1978; Guez et al. 2013). In this report, we concentrate on the contribution of CD to the neuronal basis of saccadic suppression and seek to elucidate components of its underlying brain circuitry.

A neuronal correlate of CD-driven saccadic suppression in the monkey was first identified in the superficial layers of the superior colliculus (referred to as SCs, as opposed to SCi for the intermediate layers). SCs neurons, which are visually responsive, showed suppression of spontaneous activity during and after saccades (Goldberg and Wurtz 1972; Robinson and Wurtz 1976). This suppression continued to be observed when CD was the only available signal to drive it, as shown in experiments that eliminated both visual and proprioceptive signals by measuring visual activity in complete darkness and by stopping execution of saccades with a retrobulbar block (Richmond and Wurtz 1980). Neuronal suppression with saccades was later identified in cortex, in the middle temporal area (MT), where neurons showed suppression of the visual sweep caused by saccades (Thiele et al. 2002). Subsequent experiments have verified this finding and extended it to other cortical areas (Ibbotson et al. 2007; Ibbotson et al. 2008; Bremmer et al. 2009; Crowder et al. 2009; Han et al. 2009; Watson and Krekelberg 2011; Joiner et al. 2013). Neuronal suppression has also been observed recently in the inferior pulvinar (PI), where baseline activity was suppressed during, after, and sometimes before saccades (Berman and Wurtz 2011). This PI suppression is particularly interesting in light of evidence that the identified region in PI is a relay between SCs and MT. This was established by identifying relay neurons using electrical stimulation that orthodromically activated PI neurons from SCs and antidromically activated them from MT (Berman and Wurtz 2010). This established a neuronal circuit from SCs to PI to MT identified by physiological methods, a circuit corroborated by anatomical tracing studies (Lyon et al.

Address for reprint requests and other correspondence: R. A. Berman, Laboratory of Neuropsychology, Rm. 1B80, 49 Convent Drive, Bethesda, MD 20892 (e-mail: bermanr@mail.nih.gov).

2010). Collectively, these data show neuronal suppression in the visual neurons along the circuit from SCs, through PI to MT.

Figure 1 shows this established circuit by the red arrows, which can be compared with the previously established pathway that has its origin deeper in the SC, in the saccade-related neurons within SCi. This circuit (blue pathway in Fig. 1) travels through the medial dorsal nucleus (MD) of the thalamus to the frontal eye field (FEF) in the frontal cortex. It carries a CD signal to frontal cortex for use in the control of eye movements (Sommer and Wurtz 2008), and for the perceptual compensation for the displacement of the visual image produced by every saccade (Duhamel et al. 1992; Sommer and Wurtz 2006; Cavanaugh et al. 2016). Might this CD signal also be relevant for the suppression of the retinal blur that accompanies each saccade?

In the current study, we determine the characteristics of neuronal suppression in the circuit from SCs to MT cortex by using the same experimental tests in each area. A key aspect of our comparison was to eliminate any eye movement-related alteration of the stimulus-evoked response by presenting the visual stimulus before the saccade started. Our goal was to determine whether the circuit from SCs to MT cortex (the red circuit in Fig. 1) carries a visual signal with suppression produced by a CD, just as the circuit from SCi to the frontal cortex (blue circuit in Fig. 1) carries a CD for reducing the effects of image displacement (Sommer and Wurtz 2006; Cavanaugh et al. 2016). Our neuronal recordings revealed suppression of responses to presaccadic visual stimuli that was remarkably similar in SCs, PI, and MT. The suppression was not strictly linked with saccade direction; it occurred in the visual hemifield contralateral to the recorded neuron as well as in the ipsilateral visual field, although suppression appeared earlier for contralateral than ipsilateral saccades in all three structures. This consistency of the signal along the circuit from SCs to MT led us to explore whether the neuronal suppression in MT depended at least in part on input from SC. We succeeded in testing this hypothesis in one monkey by inactivating the saccade-related neurons within SCi and then determining whether this reduced suppression in MT. It did, which

suggests that the pathway from SC contributes to the suppression observed in MT.

## METHODS

Experiments were conducted in four male macaque monkeys, OM, OZ, GE, and CK, weighing between 8 and 13 kg. Monkeys were surgically implanted with scleral search coils to measure eye position, and with an acrylic base that accommodated a recording chamber as well as a head post for immobilizing the head during experiments. All procedures were approved by the National Eye Institute Animal Care and Use Committee and complied with Public Health Service Policy on the Humane Care and Use of Laboratory Animals.

### Behavioral Tasks

Visual stimuli were projected onto a tangent screen located 57 cm in front of the monkey. A computer running REX (Hays et al. 1982) controlled stimulus presentation, reward, the recording of eye movements and neuronal activity, and the online display of results. For initial receptive field mapping and for measuring responses to directional motion, stimuli were back-projected onto the screen from a DPI projector. We used a simple fixation task to identify the neuron's receptive field in all three structures (Berman and Wurtz, 2010, 2011). When feasible, this same task was used to characterize directional tuning of MT neurons using a random-dot motion pattern scaled for eccentricity.

For the saccadic suppression task, which required precise control of stimulus appearance and disappearance, we used galvanometers with mirrors to present brief, stationary receptive field probes. As with earlier studies of CD signals in saccadic suppression (Richmond and Wurtz 1980), testing was conducted in total darkness to eliminate background illumination that could contribute to visual masking effects. In the task (Fig. 2A), the central fixation spot and saccade targets were small red laser spots subtending  $0.4^\circ$ , and targets were positioned by galvanometers to control timing precisely. Saccade targets were often presented at  $12^\circ$  or  $15^\circ$  left or right in the visual fields contralateral or ipsilateral to the receptive field of the recorded neuron, but sometimes target locations were modified depending on receptive field location. For a subset of neurons, more than two saccade directions were tested. The probe stimulus presented in the receptive field was typically a small rectangular slit ( $1^\circ$  wide and  $5^\circ$  long). For neurons with larger receptive fields we sometimes used larger stimuli ( $2^\circ \times 10^\circ$  or  $5^\circ \times 20^\circ$ ) but we often found that the smallest was most effective. Probe luminance was either 1 or 10  $\text{cd}/\text{m}^2$ . We used the lower luminance probe in most cases, but did increase luminance if the cell responded poorly at 1  $\text{cd}/\text{m}^2$ . In some cases, we held neurons long enough to test for saccadic suppression at both luminances and observed no qualitative differences in suppression. The probe stimulus was projected onto a mirror galvanometer using a slide projector with a shutter that permitted rapid and precise presentation of the probe, thereby eliminating scattered light during the rest of the trial.

In the saccadic suppression task, trials began when the monkey attained fixation, as determined by eye position in an electronic window extending  $\pm 1.5^\circ$  from the fixation spot (Fig. 2B). After an initial fixation period of 425–625 ms, a probe stimulus was flashed in the neuron's receptive field for 10 ms while the monkey continued to fixate (*probe 1*). After a second fixation period of 800–1,200 ms, the saccade target appeared simultaneously with the offset of the central fixation spot, cueing the monkey to move its eye to the target. In a subset of experiments, we tested for suppression in trials when the saccade target appeared before this second fixation period (long before fixation offset) and found similar results; in these trials the offset of fixation likewise served as the cue for the saccade. At a variable delay after fixation spot offset (typically 150–180 ms), the

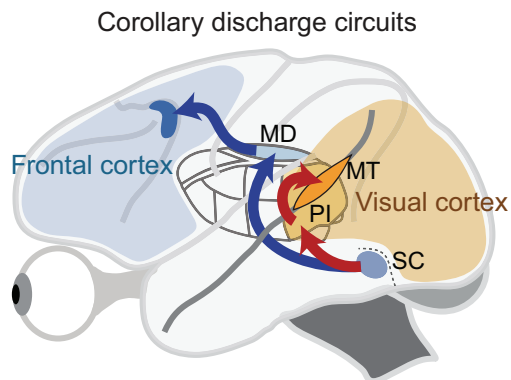


Fig. 1. A potential corollary discharge (CD) circuit in the monkey for producing saccadic suppression (red arrows). Neurons in the visual layers of the superior colliculus (SC) project to the pulvinar, with the projection centered on a subregion of the inferior pulvinar (PI). Many of these pulvinar neurons then project to the middle temporal visual area (MT) in the superior temporal sulcus of cerebral cortex. Blue arrows show a previously established pathway from the SCi saccade-related layers of SC through MD thalamus to frontal cortex, which carries a CD signal for use in the control of saccadic eye movements.

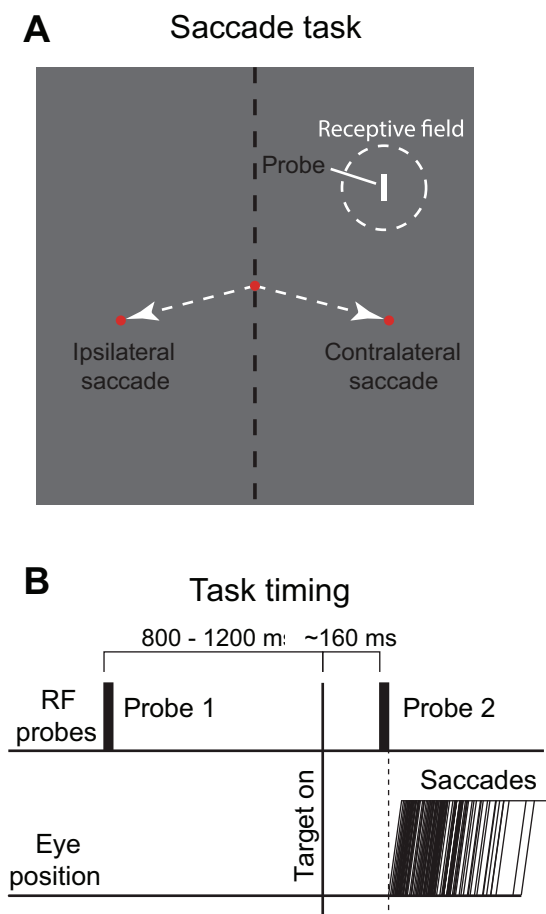


Fig. 2. Behavioral task. *A*: the monkey looked at the fixation point and then made a saccade to a target either in the same visual hemifield as the neuron's receptive field (contralateral saccade) or to a target in the opposite visual field (ipsilateral saccade). *B*: during fixation, a 10-ms stimulus (*probe 1*) was flashed in the receptive field of the neuron well before the saccade. A second 10-ms flash (*probe 2*) came on at exactly the same location in the receptive field, but immediately before saccade onset. Trials on which the saccade began before the end of *probe 2* were removed from analysis.

probe stimulus was flashed again for 10 ms in the neuron's receptive field (*probe 2*). *Probes 1* and *2* were identical—only the time of presentation varied. Timing was optimized over a series of trials to bring the onset of *probe 2* within ~200 ms before the saccade. The monkey's task was simply to move its eyes to the location of the target, defined by an electronic window scaled to saccade amplitude. In the majority of sessions, the saccade target was extinguished as soon as the monkey's eyes left the central fixation window, to minimize any visual contamination that the target might introduce. In some cases, where the monkey's saccade performance was diminished (e.g., due to decreased motivation or large target eccentricities), the saccade target remained on through the end of the trial. To receive reward, the monkey had to maintain fixation within the target window for an additional 100–600 ms. At the end of each trial, a wide-field backlight illuminated the testing room to prevent dark adaptation.

#### Neuronal Recording from MT, PI, and SC

We recorded from neurons in MT, PI, and SC using tungsten microelectrodes advanced by a stepper microdrive. Electrodes were advanced through guide tubes placed in a 1-mm-resolution grid in the recording chambers (Crist et al. 1988). We accessed MT and PI through a single rectangular chamber that was aligned to vertical stereotaxic coordinates and centered on the midline 4 mm anterior to

the ear bars. We accessed SC through a single cylindrical chamber tilted 38° from vertical (top posterior), such that electrodes were directed anteriorly.

For MT, we recorded from four monkeys, most neurons from OM and CK and fewer from OZ and GE. Electrodes approached vertically and encountered the medial superior temporal area (MST) first. Both MT and MST contain neurons tuned for directional motion (Maunsell and Newsome 1987) and we therefore distinguished MT by three criteria: 1) restricted contralateral receptive fields that scaled with eccentricity; 2) surround suppression, such that responses were strongest for small stimuli presented within the receptive field boundaries; and 3) a predictable progression of receptive field locations as the electrode descended.

For PI, all recordings were from monkey OM in the physiologically identified relay zone linking SC and MT, which is centered on the medial subdivision, PIm (Berman and Wurtz 2010). Recordings were made at sites where relay neurons had previously been identified, and where previous evidence of saccadic suppression had been observed in this and other monkeys (Berman and Wurtz 2011). Given that the focus of the current study was on characterizing saccadic suppression, we did not seek the full identification of additional relay neurons, which would have involved the additional simultaneous placement of stimulating electrodes in both SCs and area MT. For a number of sessions involving PI recording or inactivation, however, we did microstimulate the SCs layers; this permitted identification of single neurons with SC input and verified that we were in the region of interest in PI. We also used SC stimulation while recording from area MT during PI inactivation, allowing us to identify MT neurons receiving (presumably disynaptic) input from SC. The stimulation parameters and criteria for orthodromic activation have been described previously (Berman and Wurtz, 2010). For the present experiments, we typically implanted two semichronic stimulating electrodes in the lower SCs, one rostral and one caudal, targeting portions of the visual field that we expected to encounter when recording from either PI or MT.

For SC, the angle of the recording cylinder permitted electrodes to approach SC approximately normal to its surface. Entry into the SC was unmistakable because neurons in the SCs have robust responses to visual stimuli. To determine depth within the SC and to determine field location, we used a combination of a visually guided saccade task and microstimulation. In SCs, neuronal responses to target appearance would be strong, whereas activity during the saccade would be minimal. If, however, the electrode was in the SCi layers, then the neuronal activity during the saccade would stand out. Electrode placement was also confirmed by microstimulation, using a train of biphasic pulses (0.25 ms/phase at 350 Hz for 70 ms) at various current levels. In the SCi, saccades could be evoked with stimulation currents <50  $\mu$ A. Such relatively low currents, however, do not evoke saccades in SCs, and we often increased current levels to 100–150  $\mu$ A in the SCs layers to confirm our presence there.

For neuronal recordings, we targeted the SCs layers, which are the major source of input to PI (Benevento and Fallon 1975; Harting et al. 1980), and used both task-related activity and microstimulation to determine depth within the SC. Neurons in SCs are sometimes difficult to isolate (Mayo and Sommer 2008) and in addition to isolated single neurons we included a small number of sites with multineuron activity.

The fact that both perceptual saccadic suppression (Latour 1962; Diamond et al. 2000) and neuronal suppression can begin before the saccade (Ibbotson et al. 2008; Bremmer et al. 2009) gave us an opportunity to test for suppression while the image was still stable on the retina. Our paradigm was designed to compare the visual responses to exactly the same probe flashed either long before the saccade or just before it. This provided a framework for evaluating the influence of saccadic signals from SCi on visual responses at all stages of the circuit from SCs to PI to MT. This approach also introduced at least two limitations. First, the amplitude of the suppression is greater

during the saccade than before, so we were measuring a weaker suppression that was not detectable in many neurons. Second, the brief 10-ms flash was a less than optimal visual stimulus, particularly for MT, so it did not allow us to observe the effect of suppression on more robust responses.

#### Inactivation of SC or PI While Recording from MT

To follow up on our physiological recordings, we also investigated how visual activity and saccadic suppression in MT depended on input from SC and PI. We did this by inactivating neurons in SC or PI with a local anesthetic (lidocaine) and measuring changes in MT activity before and during the inactivation. The use of lidocaine was a methodological requirement for the current experiments, which involved acute, time-delimited recording from single neurons in behaving monkeys. Lidocaine acts within minutes (much faster than muscimol) and makes it feasible to assay a single cell's responses both before and during inactivation. All injections were made using a custom-built injection syringe attached to a recording microelectrode (the "injectrode") with injection rate controlled by an independent stepper microdrive (Berman et al. 2009). Typically, our goal was to maximize the alignment of receptive field locations between structures under study. In some experiments targeting SCi layers, however, we focused on placing the injectrode at sites representing attainable saccade targets.

For inactivation of SC, our standard procedure was to position a recording electrode in MT and the injectrode above an already-characterized site in SC. We typically first advanced the electrode in MT and began searching for an MT neuron that 1) showed clear suppression with saccades, 2) was well isolated, and 3) was likely to be stable for the subsequent SC inactivation. If an MT neuron met all these criteria, we then advanced the SC injectrode to the desired depth. We determined this depth within the SC by recording and/or stimulating with a microelectrode that extended 500  $\mu\text{m}$  beyond the midpoint of the injection cannula's bevel. When we were ready to begin the inactivation, we advanced the injectrode 500  $\mu\text{m}$  to center the injection at the depth of our recording and stimulation. We injected lidocaine at a standard rate of 0.3  $\mu\text{l}$  per minute, with volumes ranging from 0.5 to 2.5  $\mu\text{l}$ .

Our SC injections targeted either the SCs visual layers or the saccade-related SCi layers. Inactivations of the SCi saccade-related layers were confirmed by reductions in peak saccadic velocity after injection. Changes in saccade velocity during lidocaine inactivations of SC were determined by visual inspection. The velocity changes were all-or-nothing, and immediately obvious (at least 100%/s) in SCi, and nonexistent in SCs, as shown in RESULTS.

For inactivation of PI, the general procedure was similar to that of SC inactivations, with the placement of both an MT recording electrode as well as a PI injectrode at the start of experimental sessions. Injection sites in PI consistently had visual responses in the lower visual field, with eccentricities of 10–25°. Due to the limited number of trials the monkey would perform in a session, we did not conduct a complete characterization of the PI inactivation site before each inactivation, but rather characterized these sites before and after inactivation sessions, using receptive field mapping and orthodromic stimulation with semichronic stimulating electrodes in SC (see above for details). However, during several inactivation experiments we stimulated in either the SC or through the PI injectrode, and in each case the activation indicated that the recorded MT cell received ascending input. We used larger volumes of lidocaine in PI than in the SC, injecting either 2.5 or 4  $\mu\text{l}$  at predetermined depths based on previous detailed characterizations of the injection sites. We chose these larger volumes because 1) we did not mind the spread here so much as in SC, given that the relay zone was known to have clear visual activity but scarce saccade-related activity (Berman and Wurtz, 2011), and 2) the additional volume helped to compensate for the less direct receptive field localization. The rate of injection was higher

than for SC inactivations, at 0.6  $\mu\text{l}$  per minute in PI, so that the injection was complete within a similarly short time period.

#### Determination of Response Characteristics

*Visual response latency.* Visual responses to the probes were calculated by aligning spikes to the time of probe onset. Resulting spike histograms were smoothed by a Gaussian kernel with a 4-ms SD. Response histograms were then fit to a modified cumulative Gaussian curve to model response onset:

$$R(t) = \alpha + c \cdot \text{erf}\left(\frac{t - \mu}{\sigma\sqrt{2}}\right) \quad (1)$$

in which  $R(t)$  is the response over time,  $\alpha$  is a baseline,  $c$  is a scaling factor, and  $\mu$  and  $\sigma$  are the mean and SD of the Gaussian, respectively. The error function,  $\text{erf}(x)$ , is defined in its standard manner as:

$$\text{erf}(x) = \frac{1}{\sqrt{\pi}} \int_{-x}^x e^{-v^2} dv \quad (2)$$

Once we obtained the fit curve, we determined the latency of the response as the time at which the fitted curve reached 10% of its maximum value.

*Calculation of response amplitudes.* We used a single response epoch for each neuron, beginning 10 ms before the *probe 1* visual response latency (as determined above) and ending at a time determined separately for each neuron by visual inspection of response histograms. This same response epoch was used to calculate mean *probe 1* and *probe 2* responses. This method captured differences in *probe 1* and *probe 2* responses throughout the entire response epoch and was not susceptible to small differences in response latencies between *probe 1* and *probe 2*.

During many experiments, the target was extinguished as the saccade began, thus the saccade occurred in complete darkness. In other cases, the saccade occurred in darkness but the small red laser target light remained on and could have been swept near the receptive field by the saccade. We checked that saccades made in the presence of the target did not have an effect on neuronal activity by comparing the responses on two types of trials: those that might show such contamination, and those for which contamination was not possible (considering the time of the saccade and the latency of the neuron's visual response). We did observe some differences in *probe 2* responses between the two groups of trials, but such differences were also observed when there was no saccade target present. The response variations in both cases were not significantly different ( $P \geq 0.17$ ,  $t$ -test), and we concluded that the presence of the small target point during the saccade had no effect on *probe 2* responses. This conclusion held for all three areas studied.

*Saccade-aligned activity.* Analysis requiring the alignment of neuronal activity to saccade onset presented a small challenge. Not only did the time vary between *probe 2* and the saccade, but the time between *probe 1* and *probe 2* also varied between trials. If we were to simply align the *probe 1* responses to the saccade and align the *probe 2* responses to the saccade, these responses would be shifted in time by different amounts on each trial, resulting in erroneous comparisons between *probe 1* and *probe 2*. To assess the saccade-aligned time course of suppression, it was necessary to directly compare responses to *probe 1* with those to *probe 2*. Therefore, the alignment entailed two steps for each trial: *probe 2* responses were aligned to the saccade (shifting them on each trial by the time between *probe 2* and saccade onset), and then *probe 1* responses were aligned to the shifted *probe 2*. These steps yielded saccade-aligned *probe 1* and *probe 2* responses that could be directly compared. For each neuron, saccade-aligned responses were then normalized by the mean *probe 1* response, and finally smoothed with a Gaussian filter with a 5-ms SD.

**Statistical significance of values.** Before testing for significance, we first determined whether population values were normally distributed using a Lilliefors test for normality. For single-valued samples, we used a *t*-test if the distribution was normally distributed, and a Wilcoxon signed-rank test otherwise. For differences between two distributions, if either distribution failed the Lilliefors test for normality (at a significance level of  $P = 0.05$ ), we used a nonparametric test to compare them (Wilcoxon signed-rank test if the data were paired, Wilcoxon rank-sum test otherwise). If both distributions were normal, we used a *t*-test (paired if warranted) to determine the significance of differences between the distributions.

We examined suppression separately for ipsilateral and contralateral hemifields. Because there were individual differences between hemifields for many neurons, we concentrated on the hemifields with greatest suppression, especially when comparing among areas. Although choosing the hemifield with greatest suppression does introduce a measurement bias toward greater suppression overall, it was necessary to reveal suppression where it existed. Table 1 also contains the unbiased data for the left and right visual hemifields.

The significance of individual differences between *probe 1* and *probe 2* responses was determined by a Wilcoxon rank-sum test on the trial-by-trial spike counts within each response epoch.

**Selectivity indices.** To assess the selectivity of suppression of *probe 2* responses as a function of saccade direction, we first flipped the sign on the suppression measurement, thereby treating response reductions as positive values. We then calculated a selectivity index (Leventhal et al. 1995; Cavanaugh et al. 2002) by treating each mean value as a vector, and summing these vectors. We then normalized this vector sum by the sum of the magnitudes of each of the individual vectors. This yielded a vector pointing in the direction of greatest suppression overall, with a length between zero and one representing the selectivity of the suppression. If all directions were suppressed equally, the vector would have length zero. If there was suppression in one direction only, the vector would have length one.

To determine the significance of this selectivity measure, we performed a bootstrap test. For each data point, we separated its direction and magnitude. We scrambled the directions and calculated the length of the resulting random selectivity vector. We did this  $10^6$  times and accumulated a distribution of randomly generated selectivities. We compared the measured selectivity against this randomly generated distribution and determined how often the random selec-

tivities exceeded the measured selectivity. This determined the *P* value for significance of the measured selectivity. For example, if only 1% of the randomly generated selectivities exceeded the actual measured selectivity, the *P* value would be 0.01.

## RESULTS

We recorded from each stage along the identified circuit from SCs through PI to MT (Fig. 1, red pathway) to test for a neuronal correlate of saccadic suppression driven by corollary discharge signals. While the monkey fixated, we recorded the neuronal responses to two 10-ms flashes in the receptive field of a neuron. Both flashes appeared before a saccade was made to a target outside the receptive field either in the same visual hemifield as the receptive field or the opposite hemifield (Fig. 2A). The first flash was presented long before the saccade (visual *probe 1*) and the second, identical 10-ms flash appeared just before the saccade (*probe 2*, Fig. 2B). Both *probe 1* and *probe 2* were presented in the neuron's receptive field while the monkey's eyes were not moving; the key difference was that a saccade was imminent in the case of *probe 2* but not *probe 1*, allowing us to observe the influence of a saccadic CD on visual responses (see *Behavioral Tasks*).

### Suppression in MT

We first investigated saccadic suppression in area MT. Figure 3A shows the response of an example MT neuron to *probe 1* (left) and the responses to contralateral and ipsilateral *probe 2* (right). Responses to *probe 2* are markedly reduced compared with those to *probe 1*, indicating suppression for visual stimuli appearing just before the saccade. Note that this neuronal suppression was not strongly dependent on the laterality of saccade direction: suppression occurred for responses before saccades to both the contralateral (solid trace) and ipsilateral (dashed trace) hemifield.

The suppression of visual responses is evident in the sample of 80 MT neurons recorded in monkey OM (Fig. 3B). Probe-aligned responses to *probe 1* are shown on the *x*-axis, *probe 2*

Table 1. Unbiased data for left and right visual hemifields

| Monkey   | No. of Units | Best of Contra, Ipsi |                        | Contralateral |                        | Ipsilateral |                        |
|--|--------------|----------------------|------------------------|---------------|------------------------|-------------|------------------------|
|  |              | Suppression          | Proportion Significant | Suppression   | Proportion Significant | Suppression | Proportion Significant |
| <i>Middle Temporal Visual Area (MT)</i>              |              |                      |                        |               |                        |             |                        |
| OM   | 80           | -0.266§              | 0.64                   | -0.197§       | 0.56                   | -0.148§     | 0.46                   |
| OZ   | 39           | -0.236§              | 0.56                   | -0.140*       | 0.41                   | -0.083      | 0.49                   |
| GE   | 5            | -0.176               | 0.60                   | -0.060        | 0.40                   | -0.103      | 0.20                   |
| CK   | 37           | -0.150‡              | 0.73                   | -0.021        | 0.59                   | -0.096*     | 0.49                   |
| Total  | 161          | -0.230§              | 0.64                   | -0.139§       | 0.53                   | -0.119§     | 0.47                   |
| <i>Inferior Pulvinar (PI)</i>                        |              |                      |                        |               |                        |             |                        |
| OM   | 32           | -0.204‡              | 0.44                   | -0.109        | 0.31                   | -0.092      | 0.34                   |
| OZ   |              |                      |                        |               |                        |             |                        |
| GE   |              |                      |                        |               |                        |             |                        |
| CK   |              |                      |                        |               |                        |             |                        |
| Total  | 32           | -0.204‡              | 0.44                   | -0.109        | 0.31                   | -0.092      | 0.34                   |
| <i>Superior Colliculus, Superficial Layers (SCs)</i> |              |                      |                        |               |                        |             |                        |
| OM   | 22           | -0.225‡              | 0.55                   | -0.194†       | 0.50                   | -0.103*     | 0.36                   |
| OZ   | 18           | -0.067               | 0.33                   | -0.052        | 0.22                   | 0.031       | 0.17                   |
| GE   | 14           | -0.193*              | 0.50                   | -0.155        | 0.50                   | -0.122      | 0.43                   |
| CK   |              |                      |                        |               |                        |             |                        |
| Total  | 54           | -0.164§              | 0.46                   | -0.136‡       | 0.41                   | -0.063      | 0.31                   |

\* $P \leq 0.05$ , † $P \leq 0.01$ , ‡ $P \leq 0.001$ , § $P \leq 0.0001$ . Italic numerals indicate nonparametric test.

on the y-axis. There are two data points for each neuron: a square symbol for the contralateral *probe 2* response, and a circle for ipsilateral. The larger points represent the greatest suppression values for each neuron (see *Statistical significance of values*). Most responses fall below the diagonal equality

line, showing the tendency for *probe 2* responses to be suppressed, often significantly (filled symbols indicate Wilcoxon rank-sum test,  $P \leq 0.01$ ). For this monkey, suppression before saccades made to the contralateral hemifield (19.7%,  $P < 0.0001$ , *t*-test,) was greater than to the ipsilateral hemifield (14.8%,  $P < 0.0001$ , *t*-test; see Table 1). This 4.9% difference did not reach significance ( $P = 0.081$ , paired *t*-test).

Because there was suppression before saccades to both hemifields, we simply selected the largest magnitude of suppression for the two fields to characterize how much each neuron was suppressed (the large symbols in Fig. 3, *B* and *C*). Using this single value for each neuron, the mean for the maximum suppression for neurons in monkey OM was 26.6% ( $P < 0.0001$ , *t*-test; Table 1).

In the sample of 161 MT neurons recorded from all four monkeys (Fig. 3*C*), we observed a mean suppression of 23.0% ( $P < 0.0001$ , *t*-test). Again, the slight (2.0%) average difference in suppression between saccades to ipsilateral and contralateral hemifields over all four monkeys was not significant ( $P = 0.56$ , Wilcoxon signed-rank test). Details of suppression in area MT from each monkey are enumerated in Table 1.

The existence of suppression for both contraversive and ipsiversive saccades suggests that the suppression was global; in all neurons susceptible to suppression, saccades to either hemifield typically caused a reduction in activity. We attempted, however, to uncover any further selectivity by examining not just the hemifield into which the saccade was directed, but also how much the direction of the saccade differed from the location of the neuron's receptive field. We reasoned that the slightly stronger suppression for contralateral saccades might reflect selective mechanisms for saccades directed to targets nearest the neuron's receptive field.

We therefore asked whether suppression in area MT relates to the location of the neuron's receptive field (Fig. 4*A*). For this analysis, we focused on neurons with significant saccadic suppression for either hemifield (73 neurons in all four monkeys). In these plots, the thick black circle represents the neuronal response to *probe 1*, normalized to 1 for each neuron. Each point represents the *probe 2* response relative to *probe 1*, and each experiment contributed at least two points to the plot: one for each saccade direction. Points falling inside the thick central circle therefore indicate suppressed *probe 2* responses. The angular displacement of each point from zero (which is directly to the right) represents the difference in degrees between the location of the neuron's receptive field and the direction of the saccade. Therefore, points to the right of center

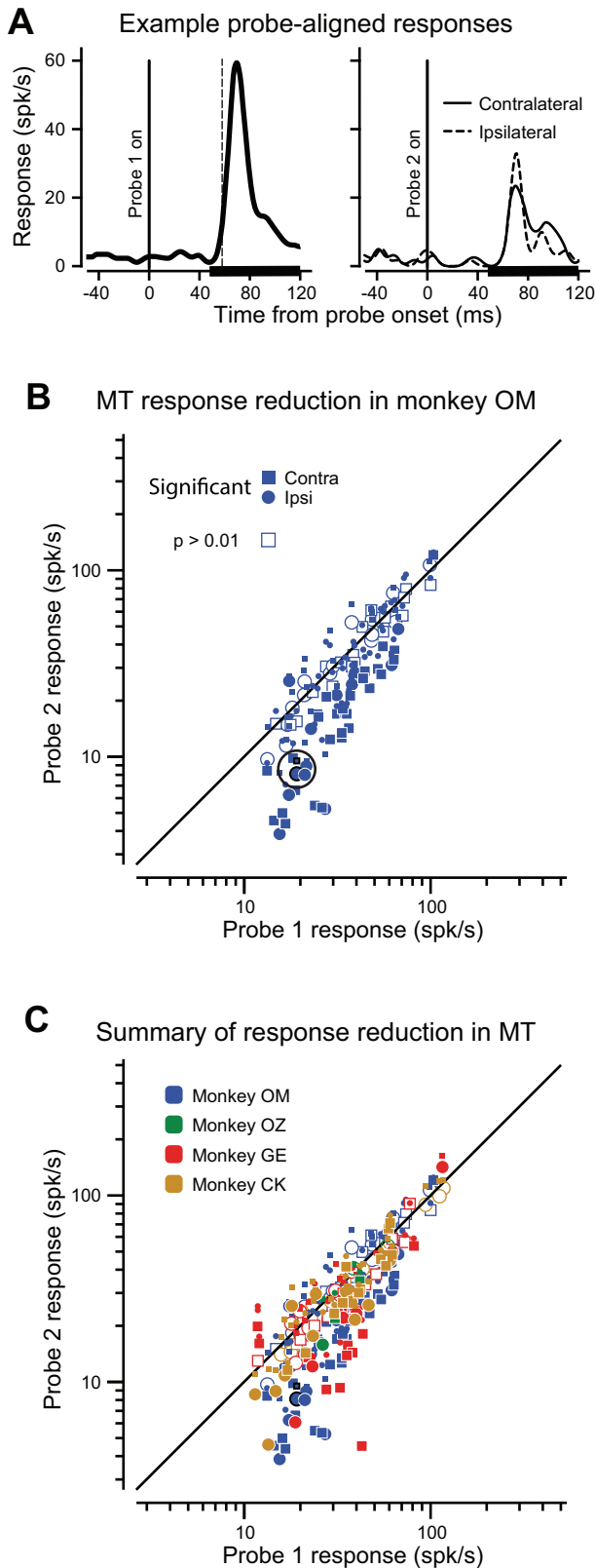


Fig. 3. Neuronal suppression in MT. *A*: an example visual response of an MT neuron to *probe 1* (181 trials) long before the saccade (*left*). The black dashed vertical line indicates the calculated visual response latency for *probe 1*. The thick black line on the x-axis shows the epoch over which mean neuronal responses were calculated. *Right*: responses to *probe 2* (solid line, 59 contralateral trials; dashed line, 59 ipsilateral trials) just before the saccade, aligned on *probe 2* onset. *B*: scatter plot of visual response amplitude for all 80 neurons in monkey OM with two points for each neuron: contralateral (square) and ipsilateral (circle) saccades. Responses of the example neuron are outlined in black. The greatest suppression for each neuron is represented by a large symbol; small symbols indicate the lesser-suppressed hemifield. Significant differences in the most suppressed hemifield are indicated by filled symbols (Wilcoxon rank-sum test,  $P \leq 0.01$ ). *C*: scatter plot of visual response amplitude for all 161 MT neurons in four monkeys. Symbol shape and shading as in Fig. 3*B*. Symbol color denotes monkey.

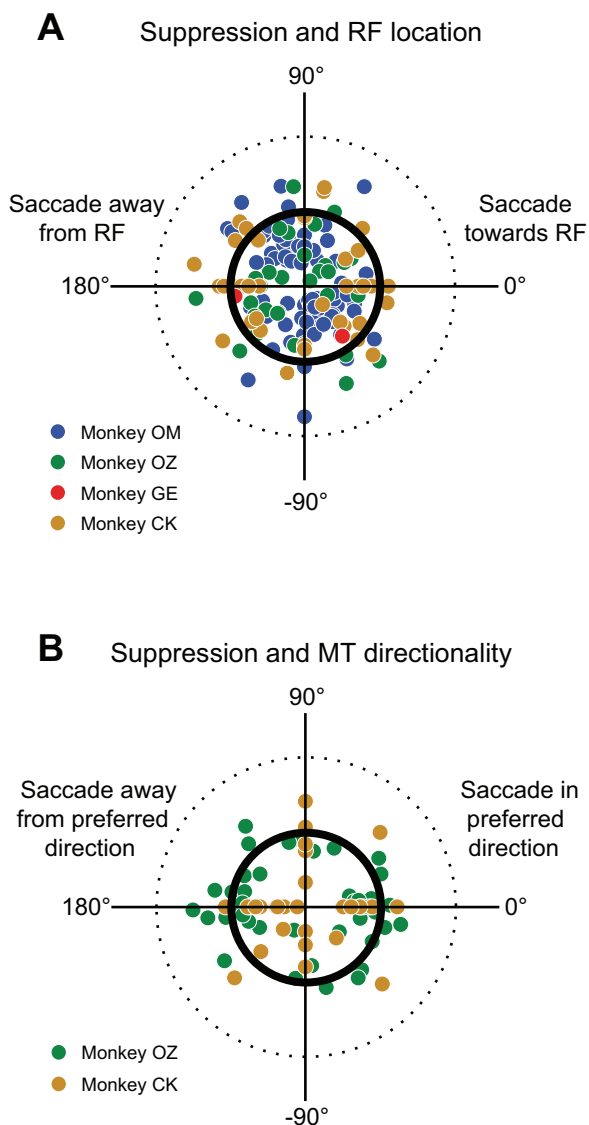


Fig. 4. Relation of suppression in MT to receptive field location and preference for motion direction. *A*: strength of suppression relative to receptive field location. Data from 73 neurons in four monkeys that had significant suppression are shown; each neuron contributes at least two data points, one for each saccade direction. The location of the receptive field for each MT neuron has been rotated so that it lies directly to the right (0°). The thick inner circle represents no difference between *probe 1* and *probe 2*, and the dashed outer circle represents a 100% response increase. Suppression is not significantly related to receptive field location. *B*: relation of suppression to preferred direction of motion for 33 MT neurons in monkeys OZ and CK. Plot is similar to that in *A*, except now the canonical direction at 0° represents the neuron's preferred direction of motion. Suppression is not dependent on directional selectivity in MT.

represent relative *probe 2* responses before saccades directed toward the neuron's receptive field, whereas points to the left are for saccades away from the neuron's receptive field. We calculated the average directional selectivity of the suppression (see *Selectivity indices*). The angle of the resulting selectivity vector indicated the overall direction of greatest suppression (relative to receptive field location) and the length of the vector (0 to 1) showed the degree of selectivity. Selectivity in MT for saccade direction was slight (0.124), but it was directed near the neuron's receptive field ( $\theta = -34^\circ$ ), although this ten-

dency was not quite significant ( $P = 0.075$ , bootstrap test). This indicates no strong and systematic relationship between the strength of suppression and the direction of the saccade relative to the neuron's receptive field.

We next asked whether the strength of suppression was related to the intrinsic directional tuning of individual MT neurons. To do so, we repeated the analysis described above, but used the MT neuron's preferred motion direction rather than the receptive field location as the reference direction at zero degrees. This analysis was performed with data from 33 neurons in two monkeys for which we either qualitatively or quantitatively determined the MT neuron's preferred motion direction. In Fig. 4*B*, the points to the right of center now represent *probe 2* responses with saccades directed in the neuron's preferred direction of motion. We calculated the overall selectivity vector and found no selectivity (selectivity = 0.116,  $\theta = 220^\circ$ ,  $P = 0.46$ , bootstrap).

These two analyses indicate that neuronal suppression in MT is not restricted to a single saccade direction nor predicted by a neuron's directional tuning. Furthermore, the absence of any relationship between MT direction preference and saccadic suppression indicates again that visual reafference had no effect on the suppression we measured. Responses for saccades causing retinal motion in a direction opposite the neuron's preference would have been lower than for those causing retinal motion in the neuron's preferred direction, resulting in measurable selectivity in Fig. 4*B*. No such relationship was observed.

To summarize, we observed suppression of visual responses in area MT just before saccade onset. Overall suppression was ~23%. This suppression was global; it was generally present for all saccade directions tested, although individual neurons could show suppression for some directions and not others. The magnitude of suppression in MT neurons was not significantly related to saccade direction toward or away from the receptive field of the neuron, or toward or away from its direction of preferred motion.

#### Suppression at Earlier Stages of the Circuit: SCs and PI

After establishing the presence of CD-driven saccadic suppression in MT, we used the same task to investigate the saccadic modulation of visual responses along the circuit from SC through PI to MT. We recorded in the identified relay zone in PI (Berman and Wurtz 2010) and in the SCs visual layers (see *Neuronal Recording from MT, PI, and SC*).

In PI, probe-aligned visual responses frequently showed suppression, as can be observed in Fig. 5*A*. Here, suppression is shown for the 32 PI neurons (blue dots) compared with all the neurons in MT (gray dots). Filled symbols show significant differences between *probe 2* and *probe 1* responses for individual PI neurons. Across the population, the reduction in *probe 2* responses was 20.4% ( $P = 0.0003$ , *t*-test), and Table 1 shows the details of the suppression in PI. As in area MT, the overall difference in suppression between ipsilateral and contralateral saccades in PI was not significant (1.6%,  $P = 0.74$ , *t*-test).

For the SCs sample in Fig. 5*B* (and Table 1), responses were recorded from 54 neurons in three monkeys. We found that *probe 2* responses were reduced 16.4% compared with *probe 1* responses ( $P < 0.0001$ , signed-rank test). Unlike areas MT and

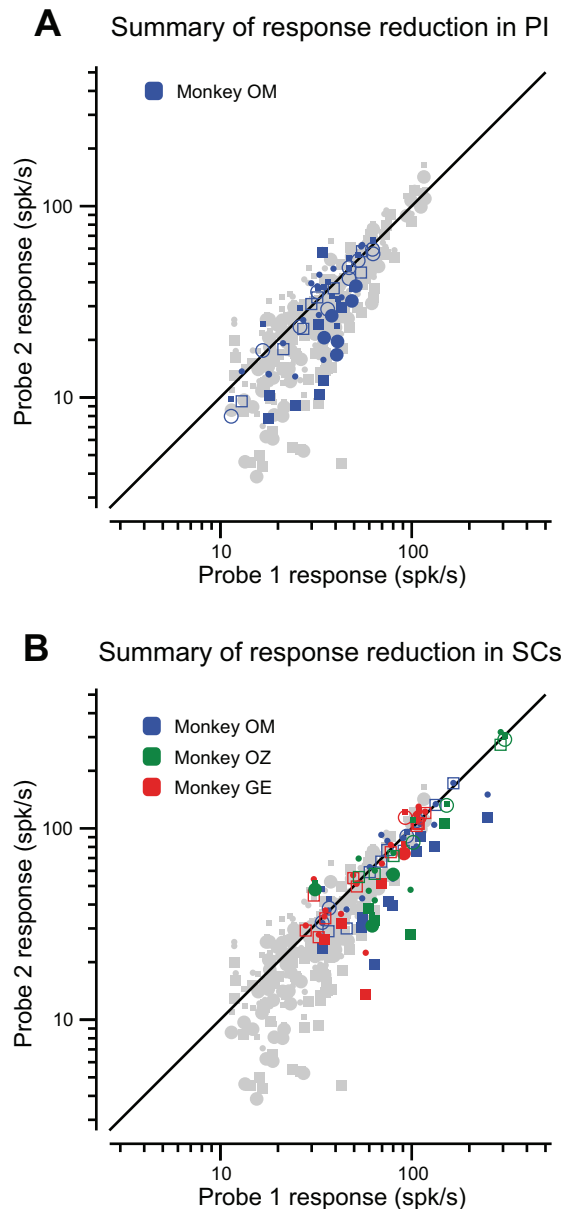


Fig. 5. Summary of suppression in PI and SC. *A*: scatter plot of 32 PI neurons in monkey OM. Symbols and markings as in Fig. 3*D*. Neurons showing suppression fall below the diagonal equality line. Filled symbols indicate significant changes in *probe 2* responses (*t*-test,  $P \leq 0.01$ ). The results from MT (Fig. 3*C*) are dimmed in the background for comparison. *B*: data for 54 units in SCs from three monkeys. Symbols and markings as in Fig. 3*C*. The points in the background are again the MT data presented for comparison.

PI, we did observe a significant difference in suppression between ipsilateral and contralateral saccades (7.3%,  $P = 0.0005$ , *t*-test), with stronger suppression for the contralateral direction.

#### Strength of Suppression Along the Path from SCs to MT

After we had established the presence of CD suppression in SCs, PI, and MT, we next directly compared two features of suppression among the three areas to determine whether there were significant, systematic changes along the ascending circuit. First, we compared the magnitude of suppression. We considered, for example, that robust differences in the magni-

tude of suppression could implicate additional modulation arising either along the circuit itself or from other brain regions. As detailed in Table 2, we found that suppression of visual responses was slightly stronger at each ascending stage of the circuit, although not significantly so, emphasizing the similarity of the suppressive signal across these areas.

Second, as we did for MT, we compared the relative strength of suppression for saccades as a function of visual hemifield in all three areas (Table 1). When we compared saccades into the contralateral and ipsilateral visual fields, we found that neither areas MT nor PI showed significant differences in suppression between hemifields, although both regions favored suppression in the contralateral hemifield. In MT, for all four monkeys combined, suppression for saccades into the contralateral hemifield was 2.0% greater than ipsilateral ( $P = 0.56$ , signed-rank test). In PI, this difference was 1.6% ( $P = 0.74$ , paired *t*-test). In contrast, suppression in SCs was significantly greater for the contralateral hemifield (7.3%,  $P = 0.0005$ ).

We also examined the strength of suppression with respect to the receptive field location, as in Fig. 4*A* for MT (see *Selectivity indices*). For this selectivity measure, we found even less significance for PI and SCs than for MT (PI selectivity = 0.20,  $P = 0.33$ ; SCs selectivity = 0.11,  $P = 0.77$ ). These data indicate that suppression of visual responses is not strictly linked to receptive field location at any point along the circuit. There is nevertheless a tendency for stronger suppression accompanying contralateral saccades, which is most evident in SCs. We consider this contralateral bias in the investigation of time courses, below.

#### Time Course of Suppression Signals Along the Path from SCs to MT

When is saccadic suppression first evident in the neuronal activities at each stage of the circuit? This question is of interest not only with respect to perceptual time courses reported previously (Latour 1962; Diamond et al. 2000), but also with respect to the comparison of timing across steps in the circuit. For the comparison, we particularly wanted to determine whether any latency differences would reject the sequence from SCs to PI to MT. For example, if we observed suppression in MT earlier than in the other areas, this would indicate a suppressive input coming from some other source than through SCs and PI. To compare the timing of suppression across areas, we aligned neuronal activity to saccade onset, rather than on probe onset as in earlier analyses (see *Saccade-aligned activity* for further details). This allowed for the comparison of *probe 1* and *probe 2* responses. As can be seen in Fig. 6, saccade-aligned responses (Fig. 6*B*) are smaller than their probe-aligned counterparts (Fig. 6*A*) because the visual activity is distributed in time around the saccade. It is nevertheless evident in the example neuron that saccade-aligned *probe 2* responses (dotted line) are reduced compared with

Table 2. Differences between areas

|                     | SC to PI | PI to MT | SC to MT |
|---------------------|----------|----------|----------|
| Suppression         | -4.0%    | -2.6%    | -6.5%    |
| Significant neurons | -2%      | +20%*    | +18%*    |

\* $P \leq 0.05$ . SC, superior colliculus; PI, inferior pulvinar; MT, middle temporal visual area. Italic numerals indicate nonparametric test.



those of *probe 1* (solid line). Although the saccade-aligned activity for single neurons was noisy due to the smaller overall responses, we reasoned that we could estimate the time course of suppression in each structure by averaging data across cells. We calculated time courses separately for each saccade direction (contralateral and ipsilateral), and a neuron contributed to the mean time course if it exhibited significant suppression ( $P \leq 0.01$ ) for that direction. We assessed the resulting suppression time courses at each stage of the circuit (MT, PI, SCs; Fig. 6, C–E). Due to the markedly different number of

data obtained in each of the three areas (as well as the different number of significant results as shown in Table 2), we could not use statistical significance as a reliable indicator of suppression onset, so we adopted another set of criteria. We first identified each point at which the suppression value first became less than zero (indicating *probe 2* < *probe 1*). The onset of suppression was then accepted as the first candidate for which 1) suppression reached at least 10%, and 2) suppression lasted at least 50 ms.

The time courses of suppression for contralateral saccades (Fig. 6, C–E, left) show that suppression began before saccade onset in all three structures. The time course from area MT (Fig. 6C) benefited from the largest data set and shows a clear divergence between *probe 1* and *probe 2* responses beginning roughly 100 ms before the beginning of the saccade and persisting more than 100 ms after saccade end. For PI (Fig. 6D) and SCs (Fig. 6E), despite fewer neurons, it is evident that suppression follows a similar time course that begins before the saccade and continues for more than 100 ms into the postsaccadic period. For ipsilateral saccades, by contrast, we found little evidence that neuronal activity diverged before saccade onset except in area MT (Fig. 6, C–E, right). In MT (Fig. 6C), where we again had the most trials for estimating the time course, we found the overall magnitude of suppression was smaller for ipsilateral than contralateral saccades and had a presaccadic onset. Time courses for PI and SCs were noisier and suggested primarily postsaccadic suppression in the ipsilateral hemifield. These data indicate that suppression begins earlier for contralateral than for ipsilateral saccades, and suggest minimal differences in the timing of suppression along the ascending pathway from SCs to MT.

#### Suppression Is Related to the Saccade

Saccadic suppression appears to be present at each stage of the identified circuit. To confirm that this suppression is driven by a CD related to the saccade, we now rule out two alternative explanations for the observed suppression. The first possibility is that response adaptation might contribute to the reduced *probe 2* responses; *probe 2* responses may be reduced simply because they appear after *probe 1*; no saccade necessary. We intentionally used interprobe intervals (900–1,300 ms) that well exceeded the intervals known to produce adaptation in SCs (Dorris et al. 2002; Fecteau and Munoz 2005; Mayo and Sommer 2008; Boehnke et al. 2011) and in other dorsal-stream

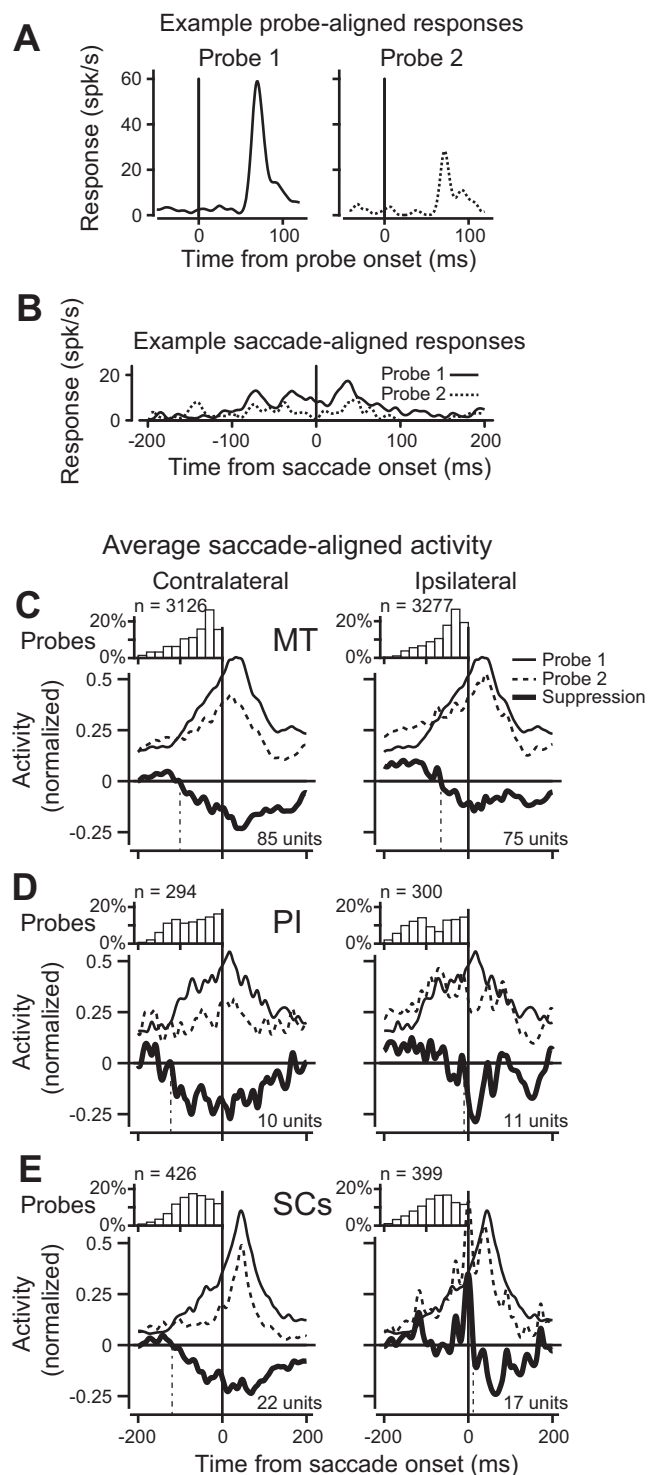


Fig. 6. Timing of saccade-aligned saccadic suppression in MT, PI, and SC. *A*: individual probe-aligned responses for the example neuron in Fig. 3. Response to *probe 1* is on the left, response to contralateral *probe 2* is on the right. *B*: same responses now aligned to the saccade. Both *probe 1* (solid) and *probe 2* (dashed) responses have been shifted in time to align with the saccade, and *probe 1* responses have been shifted in time to align with the shifted *probe 2* responses (see METHODS). *C*: normalized saccade-aligned activity averaged for all neurons with significant suppression. Data for contralateral saccades (left) and ipsilateral saccades (right). The small inset histograms show the distribution of *probe 2* offset times, with their respective counts over all included neurons. The solid black traces in the larger panels show the average saccade-aligned response to *probe 1*, dashed is for *probe 2*. The bold line is the difference between the two, and denotes suppression of *probe 2* activity over time relative to the saccade. *D*: saccadic suppression in PI. Plot elements are the same as in *C*. The relative paucity of PI data is evident in the greater variability of the data. *E*: saccadic suppression in SCs. Plot elements are the same as in *D*.

visual areas (Robinson et al. 1995; Mayo and Sommer 2008). We nevertheless confirmed the absence of adaptation effects in the current study by testing MT activity in one monkey (CR) using interleaved trials with and without saccades. We found that *probe 2* responses were decreased relative to *probe 1* responses for saccade trials (median change  $-8\%$ ,  $P < 0.05$ , Wilcoxon signed-rank test) whereas *probe 2* responses were slightly increased when no saccade was made (median change  $+8\%$ ,  $P < 0.05$ , Wilcoxon signed-rank test). The significant difference between saccade and no-saccade trials ( $P < 0.01$ , Mann-Whitney  $U$ -test), in conjunction with existing literature, demonstrate that adaptation cannot explain the present results.

Second, we asked whether our suppression findings could be due to differences in visual-response latencies between *probe 1* and *probe 2*. Although our choice of response epoch was insensitive to small variations in latency (see *Visual response latency*), large systematic differences between *probe 1* and *probe 2* responses could have had an effect on our results. However, mean differences in visual response latencies between *probe 1* and *probe 2* were small in each of the three areas ( $< 2$  ms), and were not significant ( $P \geq 0.10$ , Wilcoxon rank-sum test). This confirmed that the observed differences in response magnitude were not due to differences in the response latencies.

In summary, neuronal saccadic suppression is present at each stage in the CD circuit from SC through PI to MT. Along this circuit, the magnitude of suppression is not significantly different (Table 2), nor is its time course. Suppression of visual responses is slightly larger for saccades to the contralateral than ipsilateral visual field (significantly so for SCs), and in all areas, suppression appears earlier for contralateral saccades than for ipsilateral. The contralateral saccade-related suppression across the CD circuit is the most consistent observation.

#### Contributions of SC and PI to MT Activity

The source of the input that produces the suppression of cortical visual processing at the time of saccades has yet to be determined. One hypothesis is that the suppression originates within SC and is transmitted to the cerebral cortex. The saccade-related input that produces the SCs visual suppression could be an inhibitory input from the saccade-related SCi neurons. If so, we would expect that inactivating the different layers of SC should predictably alter the activity of MT neurons. We therefore attempted to inactivate SC neurons while we isolated and held an MT neuron to compare the change in MT activity between control and inactivation periods (see *Inactivation of SC or PI While Recording from MT*). We succeeded in one monkey, although we attempted the experiment in two others.

In our inactivation experiments, we first found a well-isolated MT neuron, then advanced an injectrode into a region of the SC; we determined the target layers in the SC for the injection by recording neuronal activity and by microstimulation using an electrode attached to the injection needle (see *Inactivation of SC or PI While Recording from MT*). Note that to test the effect of inactivation on suppression in single neurons, this experiment necessarily focused on the robust probe-aligned responses (not the saccade-aligned responses in Fig. 6). We conducted a total of 16 SC injections in monkey OM, and 10 of these met our criteria for analysis: uninterrupted

behavioral performance, and stable single-neuron isolation in MT before, during, and after the SC injection.

We found that inactivating the SC did modify suppression in MT, but across neurons there was a range of modulation. We sought to determine why the suppression varied among neurons by first considering the target of the injections: SCi or SCs. In addition to the targeting criteria described above, we confirmed the inactivated layers by measuring changes in peak saccade velocity during each injection. Velocity changes fell into two distinct groups: one in which the peak velocity clearly dropped (at least  $100^\circ/\text{s}$ ), which confirmed inactivation of SCi (Hikosaka and Wurtz 1986; Cavanaugh et al. 2012), and a second group with no injection-related velocity change, indicating that SCi was not being inactivated, and confirming the presence of the injectrode in SCs. We found a difference in modulation of suppression in MT between the experiments in these two groups. With SCi inactivation we tended to observe a reduction of suppression in MT, whereas SCs inactivations did not decrease suppression in MT, as illustrated in Fig. 7.

Figure 7A shows peak saccade velocity for each trial over time for an example experiment for both contraversive (black squares) and ipsiversive (gray circles) saccades. The obvious reduction in saccade velocity in the contralateral hemifield during the injection confirms inactivation of SCi. Figure 7B shows *probe 1* (solid) and *probe 2* (dotted) responses before (left) and during (right) SC inactivation. Before inactivation (Fig. 7B, left) suppression of the *probe 2* response was dramatic (compare solid and dotted lines). During SCi inactivation the response to *probe 1* is relatively unchanged, whereas the response to *probe 2* increases, resulting in a reduction of suppression near the time of the saccade. This is what we would expect if saccadic suppression in MT depended on an ascending suppressive signal from SCi.

Figure 7, C and D, illustrates the effect of SCs inactivation on MT activity. Here, the suppressive signal from SCi would remain unaffected (Fig. 7C, no velocity change) and the inactivation would instead affect the superficial layers. We might now expect changes in the visual responses of MT, but no change in suppression. In this example, SCs inactivation changed the visual responses to *probes 1* and *2*, but suppression of the *probe 2* response was largely unchanged (Fig. 7D). These two examples show a clear difference between the two SC subdivisions; in our overall results, however, we observed a range of changes in both nonoverlapping velocity groups.

Across our sample of 10 successful SC inactivations, we observed injections that produced changes in MT visual responses that were consistent with the examples shown in Fig. 7, B and D, but we also observed variations. With SCs inactivations, for example, the visual responses were not systematically decreased as they were for the neuron in Fig. 7D. These variations were expected, given that we had no control over the actual spread of the lidocaine, and we were not surprised to sometimes observe changes in responses to both *probe 1* and *probe 2* during experiments. As intended, our assay of suppression derives from a comparison of the two responses (to *probe 1* and *probe 2*), so we were able to observe changes in suppression irrespective of the individual changes in *probe 1* and *probe 2* responses. Our first step in quantifying results from the sample of SC inactivations was to segregate the data into contralateral and ipsilateral saccades, given that SC visual and saccadic activity are both primarily related to the

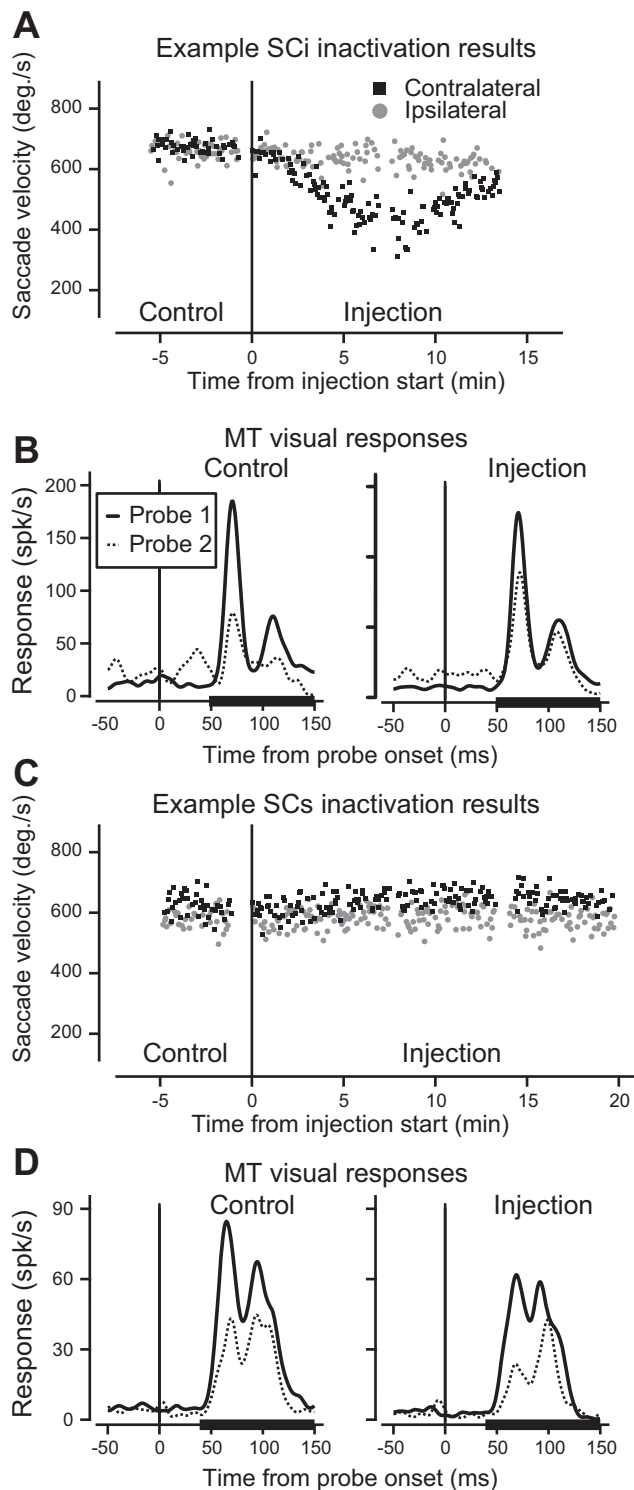


Fig. 7. Examples of the two categories SC inactivations. *A*: peak velocity of saccades toward the contralateral (black squares) and ipsilateral (gray circles) hemifields during inactivation of SCi layers. Time zero indicates the start of the lidocaine injection. *B*: responses of an MT neuron (for which saccade velocity is shown reducing in *A*). *Probe 1* responses (long before the saccade) are plotted in solid lines, *probe 2* responses (just before the saccade) are in dotted lines. The thick black lines on the *x*-axes show the epoch in which the mean neuronal responses were calculated. *C*: peak velocity of saccades during inactivation of SCs layers. In contrast to SCi inactivation, saccade velocity did not change. This was remarkably consistent across experiments. *D*: responses of the MT neuron from the inactivation portrayed in *C*. Suppression did not change.

contralateral visual field, and given the differences between hemifields already observed for both probe-aligned and saccade-aligned responses. Figure 8*A* shows changes in saccadic suppression of visual responses in MT during SC inactivation. Suppression before inactivation is shown on the *x*-axis, and suppression during inactivation is shown on the *y*-axis. We first consider the inactivations that produced a reduction in saccade velocity (solid symbols), taken as indicating inactivations of SCi layers. Red symbols indicate significant changes in sup-

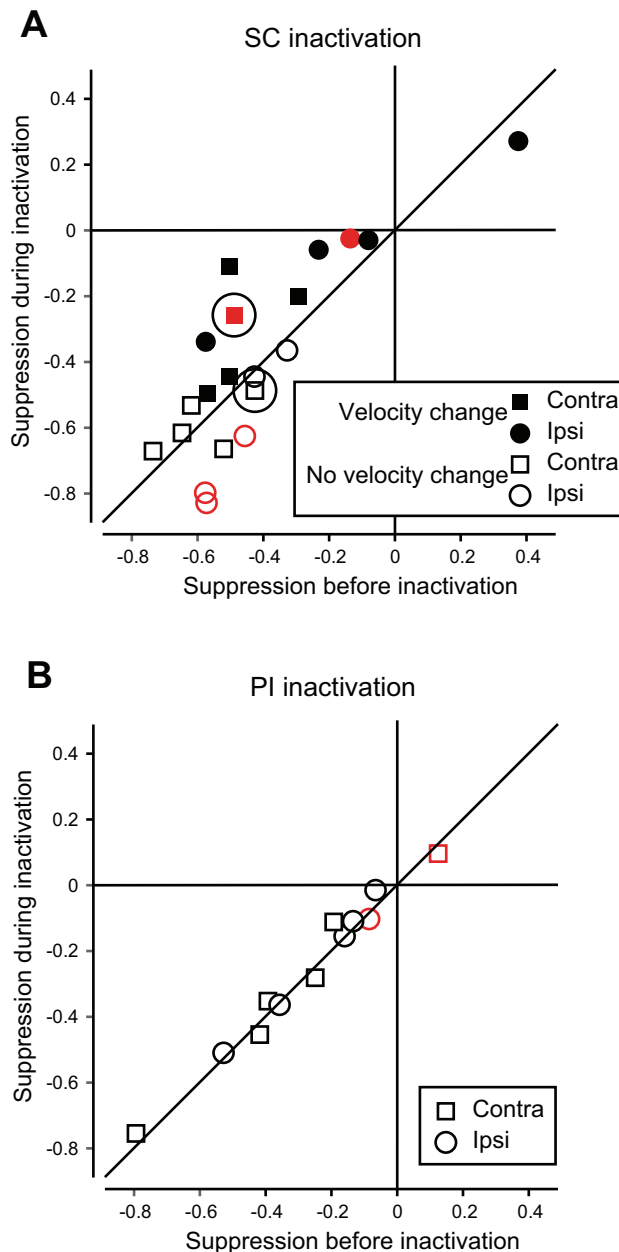


Fig. 8. Summary of effect of SC and PI inactivation on suppression of MT neurons. *A*: changes in suppression of 10 MT neurons in monkey OM during SC inactivation. Solid symbols indicate injections in which saccade velocity was reduced (SCi layers,  $n = 6$ ). Injections with no change in velocity (SCs,  $n = 4$ ) are shown with open symbols. Significant changes in suppression are indicated by red (solid for SCi, outline SCs). The two examples from Fig. 7 are circled. Points above the diagonal indicate a reduction of suppression during SC inactivation. *B*: changes in MT saccadic suppression during PI inactivation. Symbols are as in *A*. The data lie on the diagonal, indicating no change in suppression from PI inactivation.

pression ( $P \leq 0.05$ , Wilcoxon rank-sum test); squares are for contraversive saccades and circles for ipsiversive. Points on or near the diagonal indicate little change in suppression with inactivation. Points above the diagonal indicate a reduction in suppression. Most solid symbols fall above the diagonal, consistent with SCi inactivation reducing the suppressive signal (as in Fig. 7B). For injections targeting SCs, which did not reduce saccade velocity (open symbols), the data are near or below the diagonal and consistent with no reduction in saccadic suppression (as in Fig. 7D), which stands in contrast to the solid symbols from injections targeting SCi.

Saccadic suppression in MT during SCi inactivation was reduced by 8.3%, whereas inactivating SCs actually increased suppression by 5.9% ( $P = 0.11$  and  $0.21$ , respectively, Wilcoxon signed-rank test). Although the median changes in SCi and SCs did not reach significance due to the small number of inactivations, the 14.2% difference between SCi and SCs inactivation was significant ( $P = 0.018$ , Wilcoxon rank-sum test).

After SCs, PI is the next step in the circuit, and we asked how activity in area MT would be altered by inactivation of PI. Our previous work (Berman and Wurtz, 2011) suggested that PI transmits a visual signal to area MT, just as SCs transmits the visual signal to PI. Although neuronal saccadic suppression is present in PI (as in SCs), PI does not itself carry saccade-related signals (Berman and Wurtz, 2011), so there was no saccade-related activity to alter. We therefore expected that if PI inactivation had any effect on MT activity, it would be similar to SCs inactivation: a possible change in visual responses but no change in saccadic suppression. When we inactivated the identified PI relay zone, we found no systematic changes in visual responses. More critically, we observed no change in MT suppression. Figure 8B shows how all data fall on the diagonal, indicating no change in MT neuronal suppression with PI inactivation ( $-1.1\%$ ,  $P = 0.36$ , Wilcoxon signed-rank test).

In summary, although the supporting results of these SC inactivations are from a single monkey, they uphold the contribution of saccadic activity within SCi to saccadic suppression in MT. In contrast, inactivations of visual neurons both in the SCs and the PI relay did not reduce suppression. These findings are consistent with the neuronal suppression signal originating in SCi, and provide a promising basis for a more complete verification of the circuits contributing to saccadic suppression.

## DISCUSSION

### *Suppression along the SC, PI, MT Circuit*

The perceptual phenomenon of saccadic suppression, which prevents us from perceiving the visual blur that occurs during our own eye movements, exemplifies a solution to a fundamental problem: namely, distinguishing self-motion from motion in the world. This problem is solved by multiple mechanisms. The brain circuitry supporting saccadic suppression has been increasingly identified in the past half century, with studies demonstrating neuronal suppression in both cortical and subcortical areas (for reviews see Ibbotson and Krekelberg 2011; Krock and Moore 2014; and Wurtz 2008). In the present study, we concentrated on understanding CD-driven suppres-

sion in a pathway extending from the brainstem to the cortex. We measured neuronal activity in the previously identified circuit from the visual layers of SCs to PI and MT, and found evidence for saccade-related neuronal suppression at each point in the circuit. Our data demonstrate that suppression resulted from a CD of saccade preparation. The suppression was observed for probes presented just before the saccade began, and we further found that neuronal activity was suppressed starting  $\sim 100$  ms before the start of contralateral saccades. Because the eye had not started to move, the suppression cannot be due to proprioception (no muscle contraction yet) or from vision (no motion of the visual image yet). It is worth adding that in SCi, there are two broad types of neurons that could potentially provide the CD signal: burst neurons, active immediately (approximately 30–50 ms) before the saccade start, and “long-lead” or “build-up” neurons, which begin to fire more than 100 ms before saccade start (Munoz and Wurtz 1995). We do not yet know the contributions of these subtypes to saccadic suppression, but they offer a basis for suppression signals observed  $\sim 100$  ms before the saccade both in the present results and in those of earlier studies (see review by Ibbotson and Krekelberg 2011).

We have made several original observations about the CD-driven saccadic suppression along this circuit. In MT, where directional selectivity for moving stimuli is prominent, we found that suppression was unrelated to directional motion preference. More generally, suppression was not as spatially restricted as expected. When we analyzed probe-aligned responses, we found suppression for all saccade directions tested; saccades did not have to be toward the receptive field of a neuron. We nevertheless observed a contralateral bias, which was clearest at the earliest stage of the circuit, SCs. Furthermore, when we examined suppression aligned to the saccade, suppression was clearly earlier for contralateral saccades than ipsilateral saccades at each stage of the circuit. This bias is consistent with a CD-driven mechanism originating lower in the circuit, because the SC is known to have strong contralateral representations in both visual and motor domains.

We additionally observed that two other features of this suppression—its magnitude and its timing—were largely similar along the circuit from SCs to PI to MT. The suppression was about the same magnitude (16% to 23%), and suppression was consistently present at least 100 ms before the saccade in all three areas for contralateral saccades. Two exceptions to the consistency merit discussion. The frequency of neurons showing suppression varied along the circuit (44% to 64%). This variation could be related to a preferential selection of suppressed neurons in some monkeys, and inclusion of all neurons in others. Another point of variation concerned the time course of saccade-aligned suppression for ipsilateral saccades; here we observed evidence of presaccadic suppression in MT, but not in SCs or PI. This pattern suggests that whereas the CD of the saccade is responsible for suppression in the contralateral hemifield, other pathways or mechanisms probably contribute to suppression in the ipsilateral hemifield. Overall, though, the combination of our probe-aligned and saccade-aligned analyses indicated little evidence for substantive differences in CD-based saccadic suppression along the circuit from SC to MT.

### *Possible Circuit Mechanisms Connecting SC to MT*

The absence of any appreciable differences in saccadic suppression along the circuit we investigated led us to hypothesize that the neuronal suppression was established in contralateral SC and largely passed up through PI to MT. This hypothesis was derived from the correlation of suppression characteristics in all levels of the circuit. One way of going beyond correlation is to interrupt the circuit at the beginning and measure any changes in suppression at the end. In the present experiments, the beginning comprised the SCi and SCs layers.

We distinguished between SC layers using saccade velocity as an indicator of the layers affected. When saccade velocity was reduced during lidocaine injections, we took this as confirmation of inactivation of saccade-related neurons in the SCi layers (Hikosaka and Wurtz 1986; Cavanaugh et al. 2012) and its accompanying CD (Sommer and Wurtz 2004; Cavanaugh et al. 2016). Disruption of the CD signal from the SCi layers presumably reduced suppression in SCs neurons with visual responses, and this reduction of suppression was conveyed to MT. Thus, inactivation of the saccade-related activity in SCi shows that the SC contributes to the neuronal saccadic suppression in MT. In contrast, when the saccadic velocity was not reduced, it confirmed that the saccade neurons in the SCi layers were largely unaffected by the inactivation, and that the injection affected the visual neurons in the SCs layers. In this case, we found no change in saccadic suppression in MT.

When we inactivated PI, we expected to observe changes in MT that were comparable to those following inactivation of the SCs, because neurons in PI have visual responses but minimal saccade-related activity, just like SCs neurons. Suppression of MT neurons was indeed unchanged during inactivation of PI. This in itself provides substantial support for our successful targeting of SCs layers. Our findings further indicate that PI does not modify saccadic suppression, but simply conveys the suppressed responses to MT. It remains to be seen whether this particular pulvinar subdivision has a role in more active modulation of cortical activity under different task conditions, or whether it adheres to models of more classical relay functions (Cusick et al. 1993).

We unfortunately succeeded in carrying out our inactivations in only one monkey, although we tried over many months in two other monkeys. We do not regard this as a serious problem because we recorded from SC neurons that have been studied for more than 40 years, and our task examined only side effects of machine-like saccade generation. We had exceptionally good luck on the first monkey, but the demands of the experiments pushed the limits of the techniques available. Further experiments would benefit from multichannel recording in the MT to increase yield, and from the use of optogenetics to interdigitate control and experimental trials, thus eliminating failures due to loss of single neuron isolation. The optogenetic techniques we tested proved inadequate in the SC (Cavanaugh et al. 2012), but recent advances hold promise for pathway-selective manipulations (Inoue et al. 2015; Klein et al. 2016). Future experiments can also take advantage of our findings on the relatively global nature of this suppression; receptive field alignment between SC and MT need not be as meticulous as we assumed in the present experiments.

### *A Possible Complete Circuit for CD-Based Suppression from SC to MT*

The combination of the recent determination of a pathway from SC through PI to MT in the monkey (Berman and Wurtz 2010) and the neuronal suppression it shows (current results), combined with the discovery of the actions of SCi neurons on SCs neurons in rodents (Phongphanphane et al. 2011), potentially provides a complete circuit for suppression from its origins in SC to MT.

The part of this circuit derived from studies in macaque, as described here, progresses through visual neurons in SCs, then PI, and then to MT. These identified connections appear to be excitatory and convey visual activity from SCs to MT (Berman and Wurtz 2010, 2011). Until recently, the unknown part of the circuit for suppression has been the inter-layer connections within SC that might modulate visual activity. Evidence for an excitatory projection from SCi saccade-related neurons to SCs visual neurons in the rodent (Ghitani et al. 2014) indicates a mechanism for enhancement of SCs activity. But any input that suppresses the activity of SCs visual neurons would have to be an inhibitory one. Such an inhibitory connection has been identified in the rodent (Lee et al. 2007; Phongphanphane et al. 2011). Based on intracellular recordings from brain slices during stimulation of SCi neurons, they showed a suppressive signal that was conveyed from SCi to SCs by inhibitory interneurons. Critically, these interneurons receive input from a collateral of the intermediate-layer output neurons: a CD copy of the saccadic signal.

In the rodent brain slice, there is no visuomotor behavior, but instead precise microcircuit information, while in the monkey there is behavior without the precise circuit reconstruction. The combination of monkey and rodent provides a complete circuit starting from movement-generating output in the midbrain to visual processing in cerebral cortex, one of the most far reaching circuits in the mammalian brain.

Our results are consistent with the SC-PI-MT circuit conveying part of this suppression to cortex, but they cannot be taken to indicate that this circuit is the only one from SC to MT, or even from SC to other areas of cerebral cortex. Indeed, the presence of other inputs to MT (or at minimum, interhemispheric cross-talk along this ascending circuit) is suggested by our observation that saccade-aligned suppression begins earlier in MT than in SCs or PI for ipsilateral saccades. Other cortical structures with known extraretinal signals, such as the frontal eye fields (Umeno and Goldberg 1997; Joiner et al. 2013) and intraparietal areas (Duhamel et al. 1992; Bremmer et al. 2009), conceivably could contribute to MT reductions under such circumstances. Also, MT neurons presumably receive the bulk of their input from V1, which may or may not convey saccadic suppression. It remains to be seen how the circuit we present interacts with other sources of visuomotor information to produce saccadic suppression in cerebral cortex.

It is also worth noting that even within the SC, suppression of visual responses is not limited to the SCs layers, but has also been observed, with microsaccades, in the visual responses of SCi neurons (Hafed and Krauzlis 2010). In our present study, we characterized suppression in the SCs layers, and have highlighted the visual/motor distinction between the SCs/SCi layers. It is important to recognize, however, that some SCi neurons have visual as well as saccade-related activity (Wurtz

and Goldberg, 1972), and as Hafd and colleagues have demonstrated for microsaccades, these visual responses in SCi also show suppression (Hafd and Krauzlis 2010; Chen et al. 2015). Interestingly, SCi visual responses are themselves dependent upon cortical input from V1, whereas SCs responses are not (Schiller et al. 1974). It remains an interesting question whether suppression in these layers likewise relies on different inputs. The relationship between suppression in SCs and SCi, and the potential roles of intracollicular circuitry and cortical inputs for each, warrant further investigation.

Finally, to return to the brain circuits outlined in Fig. 1, it is useful to emphasize that CD-related signals are conveyed in different ways from SC to cortex. Both circuits shown in Fig. 1 start in the SCi saccade-related neurons that have collaterals carrying a CD. One circuit carries the CD to frontal cortex through MD, conveying the metrics and dynamics of the upcoming saccade. The other circuit uses the CD to suppress visual responses in SCs. This posterior circuit passes through PI to MT and carries not the CD signal itself but the suppressive consequences of the CD: an altered visual response.

### *The Role of CD-Driven Neuronal Suppression*

The CD-driven suppression we observed likely contributes to the behavioral saccadic suppression revealed by many experiments (Wurtz 2008). While the direct relationship between neuronal and perceptual suppression was beyond the scope of the present study, the magnitude of neuronal changes we observed was consistent with MT modulations known to produce perceptual effects (Tolhurst et al. 1983; Parker and Newsome 1998), and occurred on time scales consistent with behavioral observations of suppression (Ibbotson and Krekelberg 2011). It is worth considering in more detail, then, how CD-driven changes, in concert with visual masking effects, contribute during behavior. Saccadic suppression from the saccadic CD assists with elimination of the blur during saccades, and probably raises the threshold for detection during a saccade by only  $\sim 0.6$  log units of contrast (Volkman et al. 1978). On the other hand, visual masking is more powerful and can largely eliminate perception during saccades under many conditions (Matin et al. 1972; Campbell and Wurtz 1978; Volkman et al. 1978). These two mechanisms are quite different. The CD suppression is relatively weak but present with every saccade, whether in light or dark. Masking suppression is more powerful, but usually requires high-contrast visual environments.

Recent experiments by Ibbotson and collaborators (Ibbotson et al. 2007, 2008; Ibbotson and Cloherty, 2009; Cloherty et al. 2015) indicate that CD-driven neuronal suppression could be making a larger contribution to perisaccadic perception than recognized. They found that in MT and the dorsal part of MST (MSTd), neurons exhibited biphasic responses (suppression and then excitation), similar to neurons in the lateral geniculate nucleus (Ramcharan et al. 2001; Reppas et al. 2002; Royal et al. 2006) and V1 cortex (McFarland et al. 2015; see also Leopold and Logothetis, 1998 and Troncoso et al. 2015 regarding modulation by microsaccades). In MT/MSTd, responses were reduced for visual stimuli before or during the saccade (which we have observed) but were enhanced for stimuli just after the saccade (which we did not observe because our stimuli were present only before the saccade).

Ibbotson and Cloherty (2009) pointed out that relatively heightened visual sensitivity at the end of the saccade would be ideal to enhance the effective gain of any backward masking. Therefore, one major effect of CD neuronal suppression may be to enhance the strength of visual masking. This combination could greatly magnify the limited effect of the CD suppression alone, and produce saccadic omission by effectively eliminating the blur during saccades.

### ACKNOWLEDGMENTS

We are grateful to Altah Nichols and Tom Ruffner for machine shop support.

### GRANTS

Supported by the National Eye Institute Intramural Research Program at the National Institutes of Health.

### DISCLOSURES

The authors declare no competing financial interests.

### AUTHOR CONTRIBUTIONS

R.A.B. and R.H.W. conceived and designed research; R.A.B. and K.M. performed experiments; J.C. analyzed data; R.A.B., J.C., and R.H.W. interpreted results of experiments; J.C. prepared figures; R.A.B., J.C., and R.H.W. drafted manuscript; R.A.B., J.C., and R.H.W. edited and revised manuscript; R.A.B., J.C., and R.H.W. approved final version of manuscript.

### REFERENCES

- Benevento LA, Fallon JH.** The ascending projections of the superior colliculus in the rhesus monkey (*Macaca mulatta*). *J Comp Neurol* 160: 339–361, 1975. doi:10.1002/cne.901600306.
- Berman RA, Joiner WM, Cavanaugh J, Wurtz RH.** Modulation of presaccadic activity in the frontal eye field by the superior colliculus. *J Neurophysiol* 101: 2934–2942, 2009. doi:10.1152/jn.00053.2009.
- Berman RA, Wurtz RH.** Functional identification of a pulvinar path from superior colliculus to cortical area MT. *J Neurosci* 30: 6342–6354, 2010. doi:10.1523/JNEUROSCI.6176-09.2010.
- Berman RA, Wurtz RH.** Signals conveyed in the pulvinar pathway from superior colliculus to cortical area MT. *J Neurosci* 31: 373–384, 2011. doi:10.1523/JNEUROSCI.4738-10.2011.
- Boehnke SE, Berg DJ, Marino RA, Baldi PF, Itti L, Munoz DP.** Visual adaptation and novelty responses in the superior colliculus. *Eur J Neurosci* 34: 766–779, 2011. doi:10.1111/j.1460-9568.2011.07805.x.
- Bremmer F, Kubischik M, Hoffmann KP, Krekelberg B.** Neural dynamics of saccadic suppression. *J Neurosci* 29: 12374–12383, 2009. doi:10.1523/JNEUROSCI.2908-09.2009.
- Campbell FW, Wurtz RH.** Saccadic omission: why we do not see a grey-out during a saccadic eye movement. *Vision Res* 18: 1297–1303, 1978. doi:10.1016/0042-6989(78)90219-5.
- Cavanaugh J, Berman RA, Joiner WM, Wurtz RH.** Saccadic corollary discharge underlies stable visual perception. *J Neurosci* 36: 31–42, 2016. doi:10.1523/JNEUROSCI.2054-15.2016.
- Cavanaugh J, Monosov IE, McAlonan K, Berman R, Smith MK, Cao V, Wang KH, Boyden ES, Wurtz RH.** Optogenetic inactivation modifies monkey visuomotor behavior. *Neuron* 76: 901–907, 2012. doi:10.1016/j.neuron.2012.10.016.
- Cavanaugh JR, Bair W, Movshon JA.** Nature and interaction of signals from the receptive field center and surround in macaque V1 neurons. *J Neurophysiol* 88: 2530–2546, 2002. doi:10.1152/jn.00692.2001.
- Chen CY, Ignashchenkova A, Thier P, Hafd ZM.** Neuronal response gain enhancement prior to microsaccades. *Curr Biol* 25: 2065–2074, 2015. doi:10.1016/j.cub.2015.06.022.
- Cloherty SL, Crowder NA, Mustari MJ, Ibbotson MR.** Saccade-induced image motion cannot account for post-saccadic enhancement of visual processing in primate MST. *Front Syst Neurosci* 9: 122, 2015. doi:10.3389/fnsys.2015.00122.

- Crist CF, Yamasaki DS, Komatsu H, Wurtz RH.** A grid system and a microsyringe for single cell recording. *J Neurosci Methods* 26: 117–122, 1988. doi:10.1016/0165-0270(88)90160-4.
- Crowder NA, Price NS, Mustari MJ, Ibbotson MR.** Direction and contrast tuning of macaque MSTd neurons during saccades. *J Neurophysiol* 101: 3100–3107, 2009. doi:10.1152/jn.91254.2008.
- Cusick CG, Scriptor JL, Darensbourg JG, Weber JT.** Chemoarchitectonic subdivisions of the visual pulvinar in monkeys and their connective relations with the middle temporal and rostral dorsolateral visual areas, MT and DLr. *J Comp Neurol* 336: 1–30, 1993. doi:10.1002/cne.903360102.
- Diamond MR, Ross J, Morrone MC.** Extraretinal control of saccadic suppression. *J Neurosci* 20: 3449–3455, 2000.
- Dorris MC, Klein RM, Everling S, Munoz DP.** Contribution of the primate superior colliculus to inhibition of return. *J Cogn Neurosci* 14: 1256–1263, 2002. doi:10.1162/089892902760807249.
- Duhamel JR, Colby CL, Goldberg ME.** The updating of the representation of visual space in parietal cortex by intended eye movements. *Science* 255: 90–92, 1992. doi:10.1126/science.1553535.
- Fecteau JH, Munoz DP.** Correlates of capture of attention and inhibition of return across stages of visual processing. *J Cogn Neurosci* 17: 1714–1727, 2005. doi:10.1162/089892905774589235.
- Ghitani N, Bayguinov PO, Vokoun CR, McMahon S, Jackson MB, Basso MA.** Excitatory synaptic feedback from the motor layer to the sensory layers of the superior colliculus. *J Neurosci* 34: 6822–6833, 2014. doi:10.1523/JNEUROSCI.3137-13.2014.
- Goldberg ME, Wurtz RH.** Activity of superior colliculus in behaving monkey. I. Visual receptive fields of single neurons. *J Neurophysiol* 35: 542–559, 1972.
- Guez J, Morris AP, Kregelberg B.** Intrasaccadic suppression is dominated by reduced detector gain. *J Vis* 13: 1–11, 2013. doi:10.1167/13.8.4.
- Hafed ZM, Krauzlis RJ.** Microsaccadic suppression of visual bursts in the primate superior colliculus. *J Neurosci* 30: 9542–9547, 2010. doi:10.1523/JNEUROSCI.1137-10.2010.
- Han X, Xian SX, Moore T.** Dynamic sensitivity of area V4 neurons during saccade preparation. *Proc Natl Acad Sci USA* 106: 13046–13051, 2009. doi:10.1073/pnas.0902412106.
- Harting JK, Huerta MF, Frankfurter AJ, Strominger NL, Royce GJ.** Ascending pathways from the monkey superior colliculus: an autoradiographic analysis. *J Comp Neurol* 192: 853–882, 1980. doi:10.1002/cne.901920414.
- Hays AV, Richmond BJ, Optican LM.** A UNIX-based multiple process system for real-time data acquisition and control. *WESCON Conf Proc* 2: 1–10, 1982.
- Hikosaka O, Wurtz RH.** Saccadic eye movements following injection of lidocaine into the superior colliculus. *Exp Brain Res* 61: 531–539, 1986. doi:10.1007/BF00237578.
- Ibbotson M, Kregelberg B.** Visual perception and saccadic eye movements. *Curr Opin Neurobiol* 21: 553–558, 2011. doi:10.1016/j.conb.2011.05.012.
- Ibbotson MR, Cloherty SL.** Visual perception: saccadic omission—suppression or temporal masking? *Curr Biol* 19: R493–R496, 2009. doi:10.1016/j.cub.2009.05.010.
- Ibbotson MR, Crowder NA, Cloherty SL, Price NS, Mustari MJ.** Saccadic modulation of neural responses: possible roles in saccadic suppression, enhancement, and time compression. *J Neurosci* 28: 10952–10960, 2008. doi:10.1523/JNEUROSCI.3950-08.2008.
- Ibbotson MR, Price NS, Crowder NA, Ono S, Mustari MJ.** Enhanced motion sensitivity follows saccadic suppression in the superior temporal sulcus of the macaque cortex. *Cereb Cortex* 17: 1129–1138, 2007. doi:10.1093/cercor/bhl022.
- Inoue K, Takada M, Matsumoto M.** Neuronal and behavioural modulations by pathway-selective optogenetic stimulation of the primate oculomotor system. *Nat Commun* 6: 8378, 2015. doi:10.1038/ncomms9378.
- Joiner WM, Cavanaugh J, Wurtz RH.** Compression and suppression of shifting receptive field activity in frontal eye field neurons. *J Neurosci* 33: 18259–18269, 2013. doi:10.1523/JNEUROSCI.2964-13.2013.
- Klein C, Evrard HC, Shapcott KA, Haverkamp S, Logothetis NK, Schmid MC.** Cell-targeted optogenetics and electrical microstimulation reveal the primate koniocellular projection to supra-granular visual cortex. *Neuron* 90: 143–151, 2016. doi:10.1016/j.neuron.2016.02.036.
- Kregelberg B.** Saccadic suppression. *Curr Biol* 20: R228–R229, 2010. doi:10.1016/j.cub.2009.12.018.
- Krock RM, Moore T.** The influence of gaze control on visual perception: eye movements and visual stability. *Cold Spring Harb Symp Quant Biol* 79: 123–130, 2014. doi:10.1101/sqb.2014.79.024836.
- Latour PL.** Visual threshold during eye movements. *Vision Res* 2: 261–262, 1962. doi:10.1016/0042-6989(62)90031-7.
- Lee PH, Sooksawate T, Yanagawa Y, Isa K, Isa T, Hall WC.** Identity of a pathway for saccadic suppression. *Proc Natl Acad Sci USA* 104: 6824–6827, 2007. doi:10.1073/pnas.0701934104.
- Leopold DA, Logothetis NK.** Microsaccades differentially modulate neural activity in the striate and extrastriate visual cortex. *Exp Brain Res* 123: 341–345, 1998. doi:10.1007/s002210050577.
- Leventhal AG, Thompson KG, Liu D, Zhou Y, Ault SJ.** Concomitant sensitivity to orientation, direction, and color of cells in layers 2, 3, and 4 of monkey striate cortex. *J Neurosci* 15: 1808–1818, 1995.
- Lyon DC, Nassi JJ, Callaway EM.** A disinaptic relay from superior colliculus to dorsal stream visual cortex in macaque monkey. *Neuron* 65: 270–279, 2010. doi:10.1016/j.neuron.2010.01.003.
- Matin E, Clymer AB, Matin L.** Metacontrast and saccadic suppression. *Science* 178: 179–182, 1972. doi:10.1126/science.178.4057.179.
- Maunsell JH, Newsome WT.** Visual processing in monkey extrastriate cortex. *Annu Rev Neurosci* 10: 363–401, 1987. doi:10.1146/annurev.ne.10.030187.002051.
- Mayo JP, Sommer MA.** Neuronal adaptation caused by sequential visual stimulation in the frontal eye field. *J Neurophysiol* 100: 1923–1935, 2008. doi:10.1152/jn.90549.2008.
- McFarland JM, Bondy AG, Saunders RC, Cumming BG, Butts DA.** Saccadic modulation of stimulus processing in primary visual cortex. *Nat Commun* 6: 8110, 2015. doi:10.1038/ncomms9110.
- Munoz DP, Wurtz RH.** Saccade-related activity in monkey superior colliculus. I. Characteristics of burst and buildup cells. *J Neurophysiol* 73: 2313–2333, 1995.
- Parker AJ, Newsome WT.** Sense and the single neuron: probing the physiology of perception. *Annu Rev Neurosci* 21: 227–277, 1998. doi:10.1146/annurev.neuro.21.1.227.
- Phongphanhane P, Mizuno F, Lee PH, Yanagawa Y, Isa T, Hall WC.** A circuit model for saccadic suppression in the superior colliculus. *J Neurosci* 31: 1949–1954, 2011. doi:10.1523/JNEUROSCI.2305-10.2011.
- Ramcharan EJ, Gnadt JW, Sherman SM.** The effects of saccadic eye movements on the activity of geniculate relay neurons in the monkey. *Vis Neurosci* 18: 253–258, 2001. doi:10.1017/S0952523801182106.
- Reppas JB, Usrey WM, Reid RC.** Saccadic eye movements modulate visual responses in the lateral geniculate nucleus. *Neuron* 35: 961–974, 2002. doi:10.1016/S0896-6273(02)00823-1.
- Richmond BJ, Wurtz RH.** Vision during saccadic eye movements. II. A corollary discharge to monkey superior colliculus. *J Neurophysiol* 43: 1156–1167, 1980.
- Robinson DL, Bowman EM, Kertzman C.** Covert orienting of attention in macaques. II. Contributions of parietal cortex. *J Neurophysiol* 74: 698–712, 1995.
- Robinson DL, Wurtz RH.** Use of an extraretinal signal by monkey superior colliculus neurons to distinguish real from self-induced stimulus movement. *J Neurophysiol* 39: 852–870, 1976.
- Royal DW, Sáry G, Schall JD, Casagrande VA.** Correlates of motor planning and postsaccadic fixation in the macaque monkey lateral geniculate nucleus. *Exp Brain Res* 168: 62–75, 2006. doi:10.1007/s00221-005-0093-z.
- Schiller PH, Stryker M, Cynader M, Berman N.** Response characteristics of single cells in the monkey superior colliculus following ablation or cooling of visual cortex. *J Neurophysiol* 37: 181–194, 1974.
- Sommer MA, Wurtz RH.** What the brain stem tells the frontal cortex. I. Oculomotor signals sent from superior colliculus to frontal eye field via mediodorsal thalamus. *J Neurophysiol* 91: 1381–1402, 2004. doi:10.1152/jn.00738.2003.
- Sommer MA, Wurtz RH.** Influence of the thalamus on spatial visual processing in frontal cortex. *Nature* 444: 374–377, 2006. doi:10.1038/nature05279.
- Sommer MA, Wurtz RH.** Brain circuits for the internal monitoring of movements. *Annu Rev Neurosci* 31: 317–338, 2008. doi:10.1146/annurev.neuro.31.060407.125627.
- Thiele A, Henning P, Kubischik M, Hoffmann KP.** Neural mechanisms of saccadic suppression. *Science* 295: 2460–2462, 2002. doi:10.1126/science.1068788.
- Tolhurst DJ, Movshon JA, Dean AF.** The statistical reliability of signals in single neurons in cat and monkey visual cortex. *Vision Res* 23: 775–785, 1983. doi:10.1016/0042-6989(83)90200-6.
- Troncoso XG, McCamy MB, Jazi AN, Cui J, Otero-Millan J, Macknik SL, Costela FM, Martinez-Conde S.** V1 neurons respond differently to object

- motion versus motion from eye movements. *Nat Commun* 6: 8114–81124, 2015. doi:[10.1038/ncomms9114](https://doi.org/10.1038/ncomms9114).
- Umeno MM, Goldberg ME.** Spatial processing in the monkey frontal eye field. I. Predictive visual responses. *J Neurophysiol* 78: 1373–1383, 1997.
- Volkman FC, Riggs LA, White KD, Moore RK.** Contrast sensitivity during saccadic eye movements. *Vision Res* 18: 1193–1199, 1978. doi:[10.1016/0042-6989\(78\)90104-9](https://doi.org/10.1016/0042-6989(78)90104-9).
- Watson T, Krekelberg B.** An equivalent noise investigation of saccadic suppression. *J Neurosci* 31: 6535–6541, 2011. doi:[10.1523/JNEUROSCI.6255-10.2011](https://doi.org/10.1523/JNEUROSCI.6255-10.2011).
- Wurtz RH.** Neuronal mechanisms of visual stability. *Vision Res* 48: 2070–2089, 2008. doi:[10.1016/j.visres.2008.03.021](https://doi.org/10.1016/j.visres.2008.03.021).
- Wurtz RH, Goldberg ME.** Activity of superior colliculus in behaving monkey. 3. Cells discharging before eye movements. *J Neurophysiol* 35: 575–586, 1972.

